Clinical & Translational Immunology

Australian and New Zealand Society for Immunology Inc.

Clinical & Translational Immunology 2024; **13**: e70009. doi: 10.1002/cti2.70009
www.wileyonlinelibrary.com/journal/cti

ORIGINAL ARTICLE

Lymphocyte activation gene 3 served as a potential prognostic and immunological biomarker across various cancer types: a clinical and pan-cancer analysis

Yifan Liu[1,a], Yuntao Yao[1,a], Xinyue Yang[1,a], Maodong Wei[1,a], Bingnan Lu[1,a], Keqing Dong[1], Donghao Lyu[1], Yuanan Li[1], Wenbin Guan[2], Runzhi Huang[3], Guofeng Xu[1] & Xiuwu Pan[1]

[1]Department of Urology, Xinhua Hospital Affiliated to Shanghai Jiao Tong University School of Medicine, Shanghai, China
[2]Department of Pathology, Xinhua Hospital Affiliated to Shanghai Jiao Tong University School of Medicine, Shanghai, China
[3]Department of Burn Surgery, The First Affiliated Hospital of Naval Medical University, Shanghai, China

Correspondence
W Guan, Department of Pathology, Xinhua Hospital Affiliated to Shanghai Jiao Tong University School of Medicine, Shanghai 200092, China.
E-mail: celiceli02@126.com

R Huang, Department of Burn Surgery, the First Affiliated Hospital of Naval Medical University, Shanghai 200433, China.
E-mail: runzhihuang2022@163.com

G Xu and X Pan, Department of Urology, Xinhua Hospital Affiliated to Shanghai Jiao Tong University School of Medicine, Shanghai 200092, China.
E-mail: xuguofeng@xinhuamed.com.cn and panxiuwu@126.com

[a]Equal contributors and co-First authors.

Received 21 July 2024;
Revised 29 August and 18 September 2024;
Accepted 19 September 2024

doi: 10.1002/cti2.70009

Clinical & Translational Immunology 2024; **13**: e70009

Abstract

Objectives. Lymphocyte activation gene 3 (LAG3), an inhibitory receptor in T-cell activation, is a negative prognostic factor. However, its impact on tumours has yet to be comprehensively elucidated on a pan-cancer scale. Thus, we aim to reveal its role at the pan-cancer level. **Methods.** We performed IHC staining on a retrospective cohort of 370 patients. Then we assessed the prognostic effect of LAG3 using Kaplan–Meier survival analysis and multivariate Cox regression analysis. In pan-cancer analysis, we constructed competing endogenous RNA and protein–protein interaction networks, conducted gene set enrichment analysis and identified correlations between LAG3 gene expression and various factors, including clinical characteristics, tumour purity, mutations, tumour immunity and drug sensitivity across 33 cancer types. **Results.** LAG3 was expressed higher in normal kidney tissues than in tumours. A high level of LAG3 gene expression was an independent prognostic factor for OS (HR = 6.60, 95% CI = 2.43–17.90, $P < 0.001$) and PFS (HR = 3.44, 95% CI = 1.68–7.10, $P < 0.001$). In pan-cancer analysis, LAG3 exhibited robust correlations with survival and tumour stages in various cancers. Moreover, LAG3 was strongly associated with immune-related genes, proteins and signalling pathways. LAG3 gene expression was positively associated with increased infiltration of activated immune cells and decreased infiltration of several resting cells. LAG3 gene expression was associated with tumour mutation burden and microsatellite instability in multiple cancers. **Conclusion.** High LAG3 gene expression was an independent risk factor in kidney neoplasms. It also functioned as a biomarker for prognosis, TIME and immunotherapy efficacy in the pan-cancer dimension.

Keywords: biomarker, kidney neoplasm, LAG3, pan-cancer analysis, retrospective clinical study

INTRODUCTION

Lymphocyte activation gene 3 (LAG3) is a type I transmembrane protein located on activated NK and T-cell lines, mediating T-cell inhibition through its interaction with major histocompatibility complex (MHC) class II.[1] The LAG3 gene is located on chromosome 12 in humans, near the CD4 gene. LAG3 is also located alongside the T-cell receptor-CD3 complex.[2] Structurally, LAG3 contains four extracellular immunoglobulin superfamily-like domains (D1–D4), highly homologous to the structure of CD4. The D1 domain possesses an additional loop for binding with MHC class II.[3,4] For the intracellular region, two motifs are distinct and conserved. One of these is a KIEELE motif with a lysine residue. The other is a repetitive EP motif composed of a series of repetitive glutamic acid-proline dipeptides.[3,5]

LAG3 has a critical influence on tumour progression and immunotherapy. It has been found that LAG3 plays a detrimental role in melanoma,[6] pleural mesothelioma,[7] muscle-invasive bladder cancer and primary central nervous system lymphoma,[7,8] by inhibiting the proliferation, initiation, homeostasis and effects of T cells.[9–11] Research has demonstrated that targeting LAG3 is a promising treatment[12,13] and several LAG3-targeted drugs have entered clinical trials.[13,14] However, there was not enough research on the relationship between LAG3 and patient survival, the genomic features of tumours, the immune microenvironment of tumours and the efficacy of immunotherapy at the pan-cancer level.

In this study, a retrospective analysis was conducted on 370 individuals diagnosed with renal neoplasms at Xinhua Hospital. Immunohistochemistry (IHC) staining and statistical analyses were employed to assess the prognostic effect of LAG3 in renal cancers using patient specimens. Additionally, a pan-cancer study was conducted to explore the differential expression and biological characteristics of LAG3, along with its impact on survival, the tumour microenvironment and the efficacy of immunotherapy.

RESULTS

IHC staining and clinical correlation analyses with Xinhua cohort

Figure 1a and Supplementary figure 1 vividly illustrate the process of our research. Initially, we performed IHC staining and clinical analysis within the Xinhua cohort, as shown by the inclusion criteria in Figure 1b. We then conducted differential analysis, clinical analysis, signalling pathway analysis and tumour-related and immune-related analyses using external databases. Figure 1c shows that LAG3 protein expression was significantly higher in normal tissue than in tumour tissue ($P < 0.001$), and the results of IHC staining are intuitively shown in Figure 1d.

In Supplementary figure 2a, we present all the clinical information of our Xinhua cohort. Using the log-rank test, we determined the IHC staining score of 8 as the optimal cut-off value for classifying high or low LAG3 expression groups (Figure 2a). Then Kaplan–Meier survival curves are performed to demonstrate the prognostic value for both overall survival (OS) and progress-free survival (PFS) in patients with kidney neoplasms. Patients with high LAG3 gene expression had shorter OS and PFS ($P < 0.001$, Figure 2b). Then, we investigated the relationships between categorical variables and LAG3 gene expression through Chi-square tests, and the results are depicted in Figure 2c. In detail, higher LAG3 gene expression was correlated with worse OS and PFS ($P < 0.001$), a higher proportion of tumours in stages 3–4 and T2b-T4 ($P < 0.01$) and a higher probability of progression after treatment in kidney neoplasm ($P < 0.001$, Figure 2d, Supplementary figure 2b, Table 1). These results indicated that LAG3 protein was expressed differently between normal and tumour tissues and that tumours exhibited distinct clinical characteristics based on the level of LAG3 gene expression.

LAG3 was an independent prognostic factor in kidney neoplasm

We employed multivariate Cox regression and confirmed LAG3 gene expression as an independent risk factor for both OS and PFS. The hazard ratios (HRs) of high LAG3 gene expression were 6.60 (95% CI = 2.43–17.90, $P < 0.001$) and 3.44 (95% CI = 1.68–7.10, $P < 0.001$, Figure 2e) respectively. We calculated risk scores, plotted scatter plots and risk score curves, and performed Kaplan–Meier analysis ($P < 0.01$, Supplementary figure 2b), confirming the ability of risk score in the prediction of patient survival. Additionally, the individual and global Schoenfeld tests (Supplementary figure 2c, $P > 0.05$), residual plots

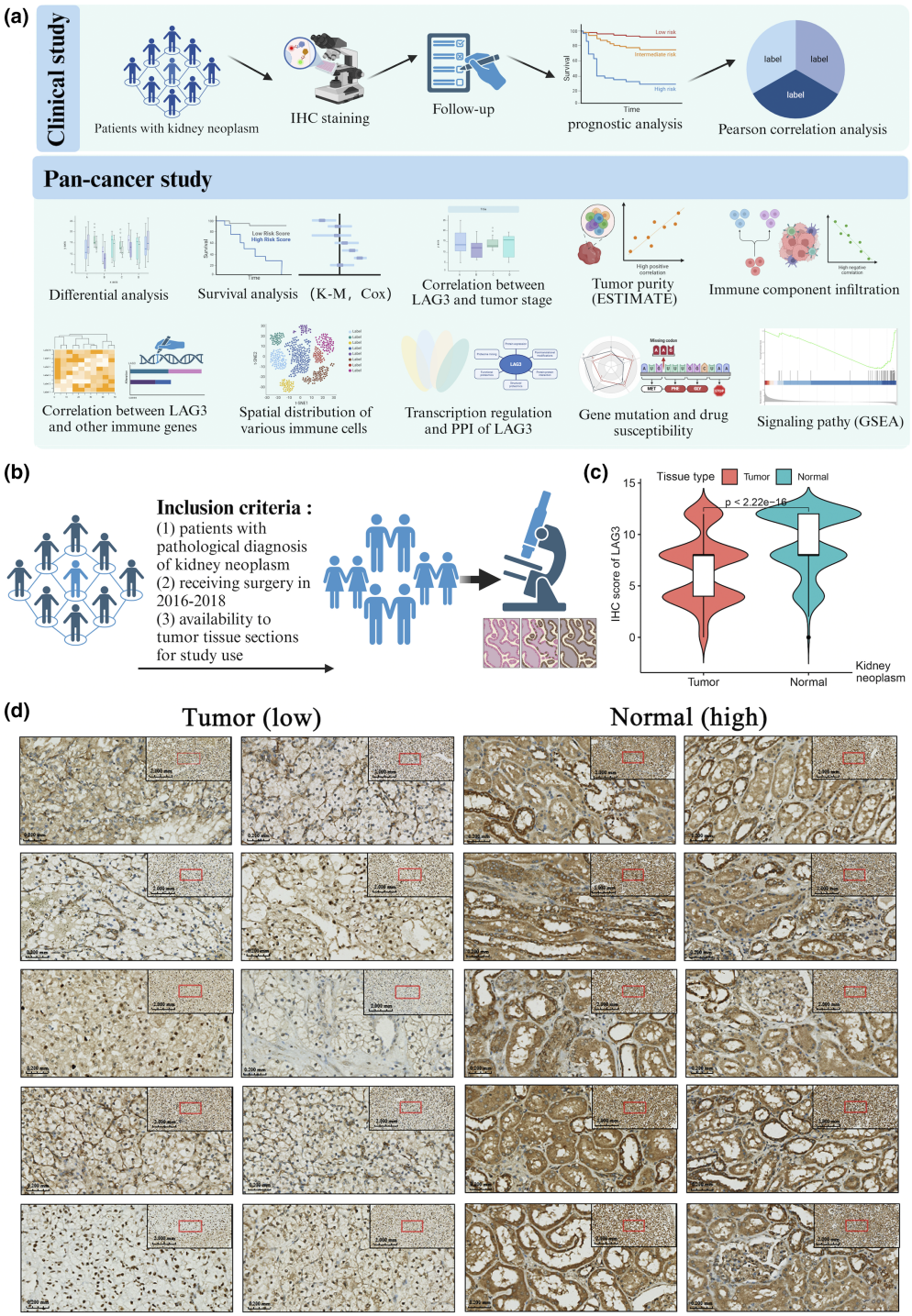

Figure 1. Procedures of statistical analyses and IHC staining. **(a)** In clinical analysis, IHC staining, follow-up, prognostic analysis and Pearson correlation analysis were performed. In pan-cancer analysis, we performed differential analysis, K-M analysis, correlation analysis, employed ESTIMATE and CIBERSORT algorithms, correlation analysis across genomics and efficacy of immunotherapy and GSEA. **(b)** The inclusion criteria of IHC staining. **(c)** The results of differential analysis across tumour and normal tissues ($P < 0.001$). **(d)** The results of IHC staining across two LAG groups. LAG3 was highly expressed in normal tissues and was relatively less detected in kidney neoplasms. CIBERSORT, cell-type identification by estimating relative subsets of RNA transcripts; ESTIMATE, estimation of stromal and Immune cells in malignant tumour tissues using expression; GSEA, gene set enrichment analysis; IHC, immunohistochemistry; K-M analysis, Kaplan–Meier survival analysis; LAG3, lymphocyte activation gene 3.

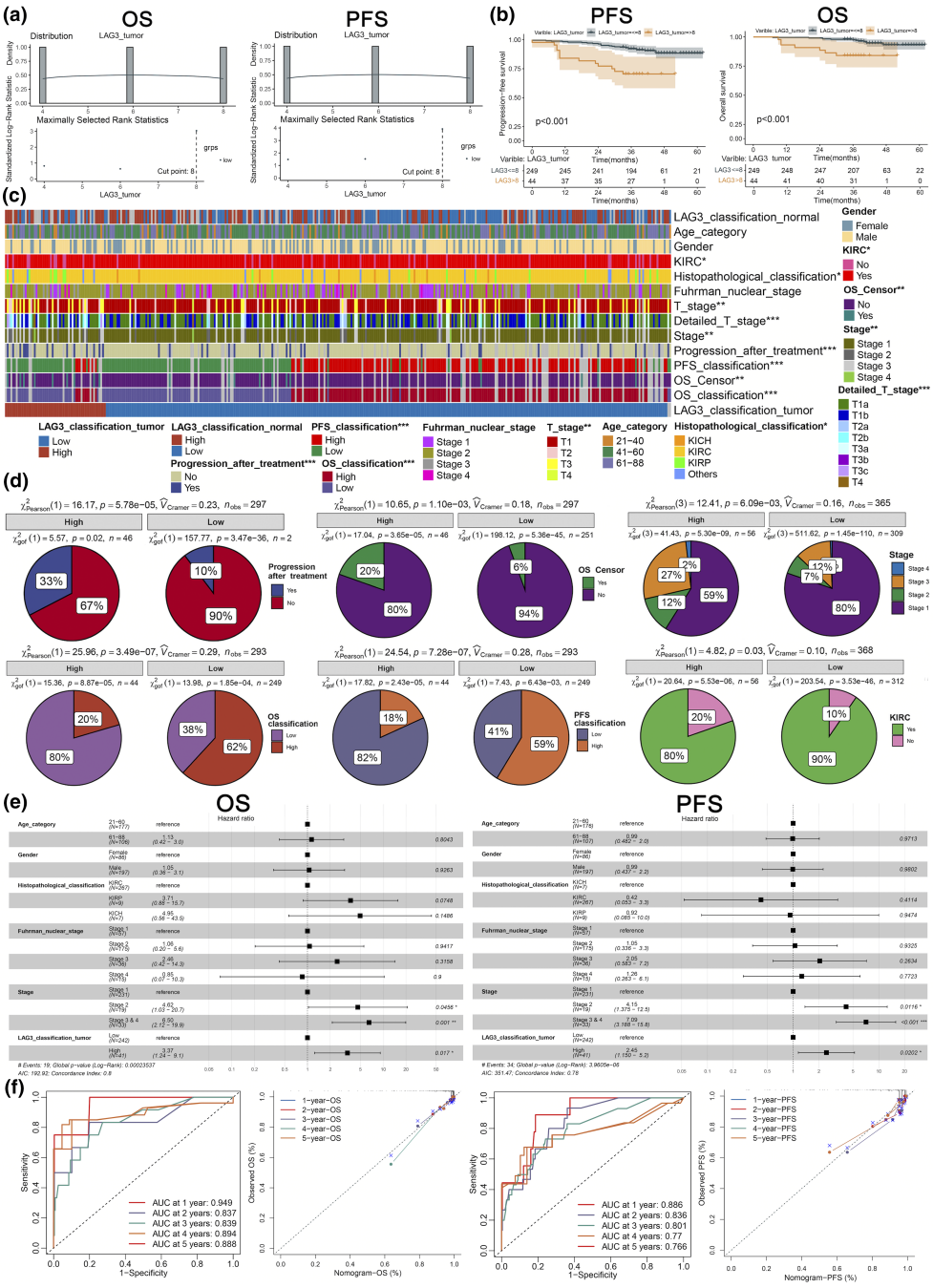

Figure 2. Correlation analyses between clinical variables and LAG3 expression. **(a)** Eight was determined as the optimal cut-off value, classifying high or low LAG3 groups. **(b)** K-M survival curve for validation of the prognostic differences in OS and PFS ($P < 0.001$). **(c)** Correlation between LAG3 expression and categorical variables. **(d)** Higher LAG3 expression correlated with worse OS ($P < 0.001$) and PFS ($P < 0.001$), a higher proportion of tumours in stages 3–4 ($P < 0.01$), a higher probability of progression after treatment ($P < 0.001$), as well as a low proportion of KIRC in all kidney neoplasms ($P < 0.05$). **(e)** The HR of high LAG3 expression were 6.60 (95% CI = 2.43–17.90, $P < 0.001$) and 3.44 (95% CI = 1.68–7.10, $P < 0.001$) in OS and PFS respectively. **(f)** The ROC and calibration curves were employed for validation of the concordance and discriminative performance. The AUC values of ROC for 1, 2, 3, 4 and 5 years of OS were 0.949, 0.837, 0839, 0.894 and 0.888, respectively, and for 1, 2, 3, 4 and 5 years PFS were 0.886, 0.836, 0.801, 0.770 and 0.766, respectively, as well as highly coincident diagonal dotted lines and solid lines in calibration curves. AUC, area under curve; HR, hazard ratio; KIRC, kidney renal clear cell carcinoma; K-M survival curve, Kaplan–Meier survival curve; LAG3, lymphocyte activation gene 3; OS, overall survival; PFS, progress-free survival; ROC, receptor operating characteristic; $*P < 0.05$; $**P < 0.01$; $***P < 0.001$.

Table 1. Demographic information and clinical characteristics of the 370 patients

Variables	Number (%)	Mean ± SD; Median (range)	*P*-value
LAG3 tumour		6.61 ± 3.16; 8 (0–12)	
LAG3 classification tumour			
NA	2 (0.54)		
Low	312 (84.32)		
High	56 (15.14)		
LAG3 normal		9.13 ± 3.05; 8 (0–12)	
LAG3 classification normal			
NA	64 (17.30)		
Low	163 (44.05)		
High	143 (38.65)		
OS censor			
Alive	276 (92.31)		0.0011*
Dead	23 (7.69)		
OS		42.24 ± 9.34; 41 (7–62)	
OS classification (months)			
High	163 (55.25)		< 0.001*
Low	132 (44.75)		
PFS		40.99 ± 10.95; 41 (0–62)	
PFS classification (months)			
High	154 (52.20)		< 0.001*
Low	141 (47.80)		
Age (category)		56.61 ± 12.45; 55 (21–88)	
21–40	33 (8.92)		
41–60	194 (52.43)		
61–88	143 (38.65)		
Gender			
Female	114 (30.81)		
Male	256 (69.19)		
KIRC			
Yes	329 (88.92)		0.03*
No	41 (11.08)		
Histopathological classification			
KIRC	328 (88.65)		0.01*
KIRP	18 (4.86)		
KICH	8 (2.16)		
Others	16 (4.32)		
Fuhrman nuclear stage			
Stage 1	69 (18.65)		
Stage 2	234 (63.24)		
Stage 3	51 (13.78)		
Stage 4	16 (4.32)		
T stage score		2.13 ± 1.54; 2 (1–8)	
T stage			
T1	282 (76.84)		< 0.01*
T2	29 (7.9)		
T3	53 (14.44)		
T4	3 (0.82)		
Detailed T stage			
1a	178 (48.5)		< 0.001*
1b	104 (28.34)		
2a	17 (4.63)		
2b	12 (3.27)		
3a	49 (13.35)		
3b	2 (0.54)		
3c	2 (0.54)		
4	3 (0.82)		

(Continued)

Table 1. Continued.

Variables	Number (%)	Mean ± SD; Median (range)	*P*-value
N stage			
Yes	2 (0.54)		
No	368 (11.08)		
M stage			
Yes	0 (0.00)		
No	370 (100.00)		
Stage			
Stage 1	282 (76.84)		< 0.01*
Stage 2	28 (7.63)		
Stage 3	54 (14.71)		
Stage 4	3 (0.82)		
Progression after treatment			
Yes	42 (14.05)		< 0.001*
No	257 (85.95)		

Variables whose *P*-value of the Chi-square tests were < 0.05 are signed with '*'.
KICH, kidney chromophobe renal cell carcinoma; KIRC, kidney renal clear cell carcinoma; KIRP, kidney renal papillary cell carcinoma; OS, overall survival; PFS, progression-free survival; SD, standard deviation.

(Supplementary figure 2d) and the concordance index for OS (0.83, 95% CI = 0.73–0.95) and PFS (0.79, 95% CI = 0.72–0.88) all proved that our models were well-validated. Nomograms were constructed to predict OS and PFS (Supplementary figure 2e), with the LAG3 classification having a significant effect on the prediction for OS and PFS (65 and 46 nomogram scores respectively). Then, the receiver operating characteristic and calibration curves confirmed the high concordance and discriminative performance of our models (Figure 2f). The areas under the curve of the receiver operating characteristic for 1, 2, 3, 4 and 5 years of OS were 0.949, 0.837, 0.839, 0.894 and 0.888 respectively (for 1, 2, 3, 4 and 5 years of PFS were 0.886, 0.836, 0.801, 0.770 and 0.766 respectively). A highly coincident diagonal dotted line and solid lines in calibration curves emerged.

Differential analysis and clinical analysis at pan-cancer level

Using the TCGA database, we first performed a differential analysis between tumour and normal tissues at the transcriptional level. Significant differences in LAG3 gene expression between tumour and normal tissues were observed in colon adenocarcinoma (COAD), glioblastoma multiforme (GBM), kidney chromophobe renal cell carcinoma (KICH), kidney renal clear cell carcinoma (KIRC), liver hepatocellular carcinoma (LIHC), lung adenocarcinoma (LUAD), uterine corpus endometrial carcinoma (UCEC), thyroid carcinoma (THCA) ($P < 0.05$, Figure 3a). We also demonstrated K-M survival curves of OS, PFS, disease-free survival (DFS) and disease-specific survival (DSS) in different cancer types between high and low LAG3 groups ($P < 0.05$, Figure 3b, Supplementary figure 3). We discovered that high LAG3 gene expression was typically associated with decreased OS in KIRC ($P < 0.001$, Figure 3b), lower grade glioma (LGG), thymoma (THYM) and uveal melanoma (UVM) ($P < 0.05$, Supplementary figure 3). Conversely, high LAG3 gene expression correlated with increased OS in ovarian serous cystadenocarcinoma (OV), skin cutaneous melanoma (SKCM) and UCEC ($P < 0.05$, Supplementary figure 3). Moreover, high LAG3 gene expression was correlated with prolonged PFS in SKCM and shortened PFS in UVM ($P < 0.05$, Supplementary figure 3). As for DFS, we found that high LAG3 gene expression was typically linked with decreased DFS in KIRC and KIRP ($P < 0.05$, Figure 3b), oesophageal carcinoma, LGG and UVM, while increased DFS was found in adrenocortical carcinoma (ACC), bladder urothelial carcinoma (BLCA), head and neck squamous cell carcinoma (HNSC), OV, THCA and UCEC ($P < 0.05$, Supplementary figure 3). In terms of DSS, high LAG3 gene expression was correlated with prolonged DSS in HNSC, OV and THCA, while shortened DSS was observed in LGG and UVM ($P < 0.05$, Supplementary figure 3). Additionally, univariate Cox regression was performed to study

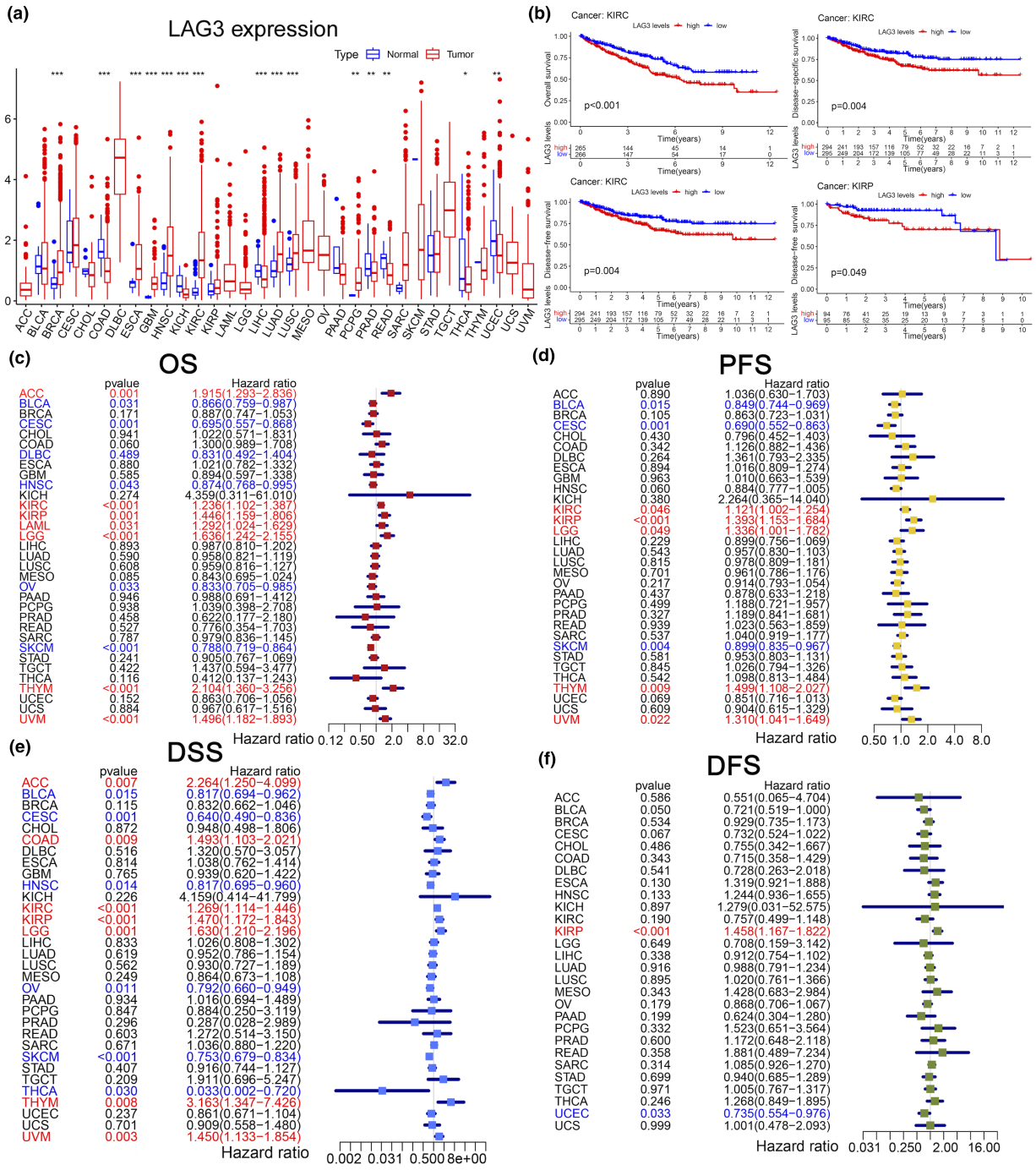

Figure 3. Differential analysis and univariate Cox regression. **(a)** Significant differences in LAG3 expression between normal and tumour tissues were observed in BRCA, COAD, ESCA, GBM, HNSC, KICH, KIRC, LIHC, LUAD, LUSC, PCPG, PRAD, READ, THCA and UCEC. **(b)** High LAG3 expression was correlated with shortened OS, DSS and DFS in KIRC ($P < 0.01$), as well as shortened DFS in KIRP ($P < 0.05$). **(c–f)** Forest plot of univariate Cox regression in OS, PFS, DSS and DFS. BRCA, breast cancer; COAD, colon adenocarcinoma; DFS, disease-free survival; DSS, disease-specific survival; ESCA, oesophageal carcinoma; GBM, glioblastoma multiforme; HNSC, head and neck squamous cell carcinoma; KIRC, kidney renal clear cell carcinoma; KIRP, kidney renal papillary cell carcinoma; LAG3, lymphocyte activation gene 3; LIHC, liver hepatocellular carcinoma; LUAD, lung adenocarcinoma; LUSC, lung squamous cell carcinoma; OS, overall survival; PCPG, pheochromocytoma and paraganglioma; PFS, progress-free survival; PRAD, prostate adenocarcinoma; READ, rectum adenocarcinoma; THCA, thyroid cancer; UCEC, uterine corpus endometrial carcinoma; $^{*}P < 0.05$; $^{**}P < 0.01$; $^{***}P < 0.001$.

the influence of LAG3 on different cancer types in the TCGA database (Figure 3c–f). For OS, high LAG3 gene expression served as a protective factor in BLCA, cervical squamous cell carcinoma and endocervical adenocarcinoma (CESC), HNSC, OV and SKCM (the HR values were 0.866, 0.695, 0.831, 0.874, 0.833 and 0.788, respectively, $P < 0.05$), while a risk factor in ACC, KIRC, KIRP, acute myeloid leukaemia (LAML), LGG, THYM and UVM (the HR values were 1.195, 1.236, 1.446, 1.292, 1.636, 2.104 and 1.496, respectively, $P < 0.05$). For PFS, high LAG3 gene expression also served as a protective factor in BLCA, CESC and SKCM (the HR values were 0.849, 0.690 and 0.899, respectively, $P < 0.05$), while a risk factor in KIRC, KIRP, LGG, THYM and UVM (the HR values were 1.121, 1.393, 1.336, 1.499 and 1.310, respectively, $P < 0.05$). For DSS, high LAG3 gene expression indicated longer DSS in BLCA, CESC, HNSC, OV, SKCM and THCA (the HR values were 0.817, 0.640, 0.817, 0.792, 0.753 and 0.033, respectively, $P < 0.05$), while shorter DSS in ACC, COAD, KIRC, KIRP, LGG, THYM and UVM (the HR values were 2.264, 1.493, 1.269, 1.470, 1.630, 3.163 and 1.450, respectively, $P < 0.05$). For DFS, only KIRP (HR = 1.458, $P < 0.001$) and UCEC (HR = 0.735, $P < 0.05$) showed significant differences. We also analysed the correlation across LAG3 gene expression and cancer stages as well as molecular subtyping (Supplementary figure 4). In KIRC, the proportion of stage three and stage four was significantly higher than stage one when LAG3 gene expression increased. In KIRP, high LAG3 gene expression was correlated with more tumours in stage three than in stage one. These results suggested that the expression of the LAG3 gene had a significant impact on both the prognosis and the tumour stage at the pan-cancer level.

Tumour purity and immune infiltration

First, we studied the relationship between LAG3 gene expression and the proportions of the three major components in the tumour tissues. Using the ESTIMATE algorithm, correlations between LAG3 gene expression and the purity of the 33 cancer types are depicted in Figure 4a and b. Specifically, positive correlations between LAG3 gene expression and the immune score were found in BLCA ($r = 0.81$, $P < 0.001$), CESC ($r = 0.8$, $P < 0.001$), KICH ($r = 0.7$, $P < 0.001$), KIRC ($r = 0.7$, $P < 0.001$), KIRP ($r = 0.7$, $P < 0.001$), LGG ($r = 0.3$, $P < 0.001$), SKCM ($r = 0.8$, $P < 0.001$), THYM ($r = 0.3$, $P < 0.001$), UCEC ($r = 0.63$, $P < 0.001$), UVM ($r = 0.8$, $P < 0.001$, Figure 4a), breast cancer (BRCA), COAD, HNSC, LIHC, LUAD, lung squamous cell carcinoma (LUSC), mesothelioma, OV and prostate adenocarcinoma (PRAD) ($P < 0.001$, Supplementary figure 5). In terms of stromal components, high LAG3 gene expression was correlated with elevated stromal scores in BLCA ($r = 0.54$, $P < 0.001$), CESC ($r = 0.4$, $P < 0.001$), KICH ($r = 0.52$, $P < 0.001$), KIRC ($r = 0.2$, $P < 0.001$), KIRP ($r = 0.50$, $P < 0.001$), LGG ($r = 0.16$, $P < 0.001$), SKCM ($r = 0.5$, $P < 0.001$), THYM ($r = 0.36$, $P < 0.001$), UCEC ($r = 0.4$, $P < 0.001$) and UVM ($r = 0.7$, $P < 0.001$, Figure 4b), as well as in BRCA, COAD, HNSC, LIHC, LUAD, LUSC, OV and PRAD (all the $P < 0.001$, Supplementary figure 5). In summary, higher LAG3 gene expression was correlated with lower tumour purity and a higher proportion of immune and stromal components.

Then, we focused on immune components and explored the infiltration of different subtypes of immune cells (Figure 4c, Supplementary figure 6). LAG3 gene expression was positively correlated with increased infiltration of $CD8^+$ T cells in UVM ($r = 0.77$, $P < 0.001$), KIRC ($r = 0.70$, $P < 0.001$), KIRP ($r = 0.62$, $P < 0.001$), SKCM ($r = 0.75$, $P < 0.001$) and COAD ($r = 0.47$, $P < 0.001$). As for NK cells, LAG3 gene expression was associated with increased infiltration of activated NK cells in several cancers, such as KIRC ($r = 0.45$, $P < 0.001$), SKCM ($r = 0.46$, $P < 0.001$) and THYM ($r = 0.34$, $P < 0.001$). Regarding regulatory T cells (Tregs), LAG3 gene expression was positively correlated with the increased cell infiltration in KIRP ($r = 0.32$, $P < 0.001$), SKCM ($r = 0.32$, $P < 0.001$) and BRCA ($r = 0.16$, $P < 0.001$). In terms of T-cell follicular helper (Tfh), LAG3 gene expression was positively correlated with the increased infiltration in KIRP ($r = 0.25$, $P < 0.001$), UVM ($r = 0.53$, $P < 0.001$), SKCM ($r = 0.17$, $P < 0.001$) and BRCA ($r = 0.21$, $P < 0.001$). For plasma cells, increased infiltration was observed with high LAG3 gene expression in KIRP ($r = 0.29$, $P < 0.001$), SKCM ($r = 0.35$, $P < 0.001$), THCA ($r = 0.56$, $P < 0.001$) and THYM ($r = 0.32$, $P < 0.001$). In THYM, BRCA, LIHC, LUAD, mesothelioma and THCA, LAG3 gene expression was correlated with increased infiltration of activated $CD4^+$ memory T cells (r value was 0.42, 0.60, 0.52, 0.39, 0.36 and 0.48, respectively, all the $P < 0.001$) while decreased infiltration of resting $CD4^+$ memory T cells (r value was −0.42, −0.29,

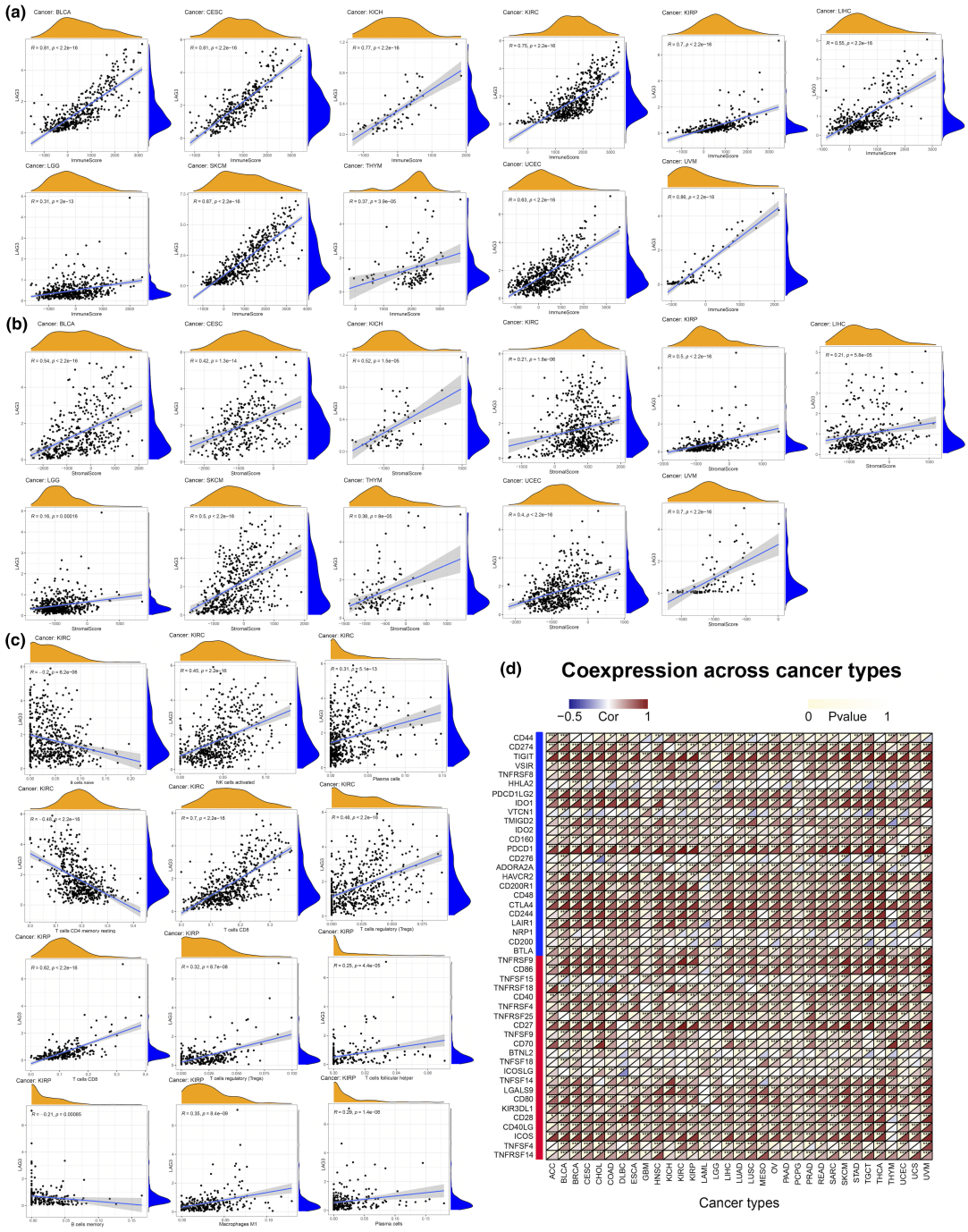

Figure 4. Immune-related analyses. **(a)** LAG3 expression was positively correlated with the immune score in BLCA, CESC, KICH, KIRC, KIRP, LGG, SKCM, THYM, UCEC and UVM. **(b)** High LAG3 expression was correlated with elevated stromal scores in BLCA, CESC, KICH, KIRC, KIRP, LGG, SKCM, THYM, UCEC and UVM. **(c)** In KIRC, LAG3 expression was negatively correlated with the infiltration of resting $CD4^+$ memory T cells, but positively correlated with activated NK cells, plasma cells, Tregs and $CD8^+$ T cells. In KIRP, LAG3 expression was associated with the infiltration of memory B cells, macrophages M1, plasma cells, Tregs, T-cell follicular helpers and $CD8^+$ T cells. **(d)** Correlation between LAG3 expression and other immune-related genes. BLCA, bladder urothelial carcinoma; CESC, cervical squamous cell carcinoma and endocervical adenocarcinoma; KICH, kidney chromophobe renal cell carcinoma; KIRC, kidney renal clear cell carcinoma; KIRP, kidney renal papillary cell carcinoma; LAG3, lymphocyte activation gene 3; LGG, brain lower grade glioma; NK cell, nature killer cell; SKCM, skin cutaneous melanoma; THYM, thymoma; Treg, regulatory T cell; UCEC, uterine corpus endometrial carcinoma; UVM, uveal melanoma.

−0.35, −0.38, −0.47 and −0.26, respectively, all the $P < 0.001$). The relationships between LAG3 gene expression and different immune cells in other cancer types (such as BLCA, CESC, OV and THYM) are demonstrated in Supplementary figure 6. In general, high LAG3 gene expression was associated with low tumour purity, specifically, increased infiltration of activated T cells and some other immune cells (such as B cells and NK cells) and decreased infiltration of resting lymphocytes along with NK cells and macrophages M1.

Additionally, results from the TIMER database are also presented for complement (Supplementary figure 7). Integrating the results of seven algorithms, LAG3 level was positively correlated with $CD8^+$ T-cell infiltration in 34 out of 40 cancer types shown. Negative correlations only appeared in THCA (TIMER and XCELL algorithms), LGG (TIMER and EPIC algorithms), KICH (EPIC algorithm), KIRP (EPIC algorithm) and THYM (TIMER, EPIC, XCELL, MCPCOUNTER and QUANTISEQ algorithms). For $CD4^+$ T cells and Tregs, most activated $CD4^+$ T cells (such as Th1, Th2 and memory-activated $CD4^+$ T cells) and Tregs infiltration were positively correlated with LAG3 gene expression in most cancers. Besides, the infiltration of activated NK cells, B cells, M1 and M2 were also positively correlated with LAG3 gene expression in most algorithms. These results were consistent with our previous findings. That was, LAG3 gene expression was correlated with increased infiltration of activated T cells and some other immune cells, as well as decreased infiltration of resting lymphocytes along with NK cells.

The distribution of the LAG3 gene in myeloid cells, T cells ($CD4^+$, $CD8^+$) and NK cells in pan-cancer single-cell transcriptional atlases is illustrated in Supplementary figures 8–10. The myeloid cells recorded in the SCDVA database did not express LAG3 (Supplementary figure 8). While in T cells of the SCDVA database, the LAG3 gene expressed higher in CD4+ T cells of $CXCL13^+$ TfhTh1 and $OAS1^+$ Treg. In $CD8^+$ T cells, LAG3 level was upregulated in $CXCL13^+$ Tex, $IFIT1^+$ ISG and $PDCD1^+$ Tex (Supplementary figure 9). Besides, LAG3 was slightly expressed in NK cells, with the median expression as 0 and was mainly identified in NK cells with markers KLRC2, NFKBIA and NR4A3 (Supplementary figure 10).

T-cell dysfunction and immune-related genes

The TIDE database was employed to evaluate T-cell dysfunction and exclusion. The results are demonstrated in Supplementary figures 11, 12. Specifically, LAG3 gene expression was positively correlated with cytotoxic T lymphocyte (CTL) level in various cancers (Supplementary figure 11). In detail, LAG3 gene expression was positively associated with CTL infiltration in BLCA ($r = 0.765$, $P < 0.05$), CESC ($r = 0.736$, $P < 0.05$), GBM ($r = 0.345$, $P < 0.05$), HNSC ($r = 0.916$, $P < 0.05$), KIRC ($r = 0.907$, $P < 0.05$), KIRP ($r = 0.953$, $P < 0.05$), LAML ($r = 0.58$, $P < 0.05$), LIHC ($r = 0.884$, $P < 0.05$), LUAD ($r = 0.779$, $P < 0.05$), LUSC ($r = 0.793$, $P < 0.05$), OV ($r = 0.662$, $P < 0.05$), PRAD ($r = 0.68$, $P < 0.05$), BRCA ($r = 0.876$, $P < 0.05$), stomach adenocarcinoma (STAD) ($r = 0.76$, $P < 0.05$) and UVM ($r = 0.973$, $P < 0.05$). Then LAG3 level was found to be positively linked with the T-cell dysfunction score for many cancers in different databases, including KIRC ($r = 3.14$, $P < 0.002$), KIRP ($r = -2.4$, $P < 0.05$), BRCA ($r = 2.31$, $P < 0.05$), HNSC ($r = 2.17$, $P < 0.05$), SKCM ($r = 2.46$, $P < 0.05$), LAML ($r = 3.69$, $P < 0.001$), LIHC ($r = 3.05$, $P < 0.05$) and LUAD ($r = 2.57$, $P < 0.05$). Furthermore, we found that in the high LAG3 group, a high level of CTL infiltration was linked with an unfavourable prognosis in these cancers except SKCM (Supplementary figure 12). These findings meant that the LAG3 gene held a close link with CTL infiltration and dysfunction, which played a significant role in the prognosis.

Figure 4d demonstrates the relationships between LAG3 expression level and immune gene expression in 33 cancer types. Most of those immune genes showed a positive correlation with LAG3 ($P < 0.05$) in the 33 cancer types. Specifically in renal cancers, LAG3 gene expression was positively correlated with CD44, TIGIT, VSIR, TNFRSF8, PDCD1LG2, TMIGD2, IDO2, CD160, PDCD1, HAVCR2, CD200R1, CD48, CTLA4, CD244, LAIR1, TNFRSF9, CD86, TNFRSF18, TNFRSF25, CD27, TNFSF9, CD70, TNFSF14, LGALS9, CD80, CD28, CD40LG and ICOS. In UVM, LAG3 gene expression was positively correlated with 38 genes, with the exception of CD44, HHLA2, VTCN1, TMIGD2, ADORA2A, CD200, CD40 and BTNL2. The close association between LAG3 and numerous immune-related genes indicated that LAG3 played a significant role in immunity.

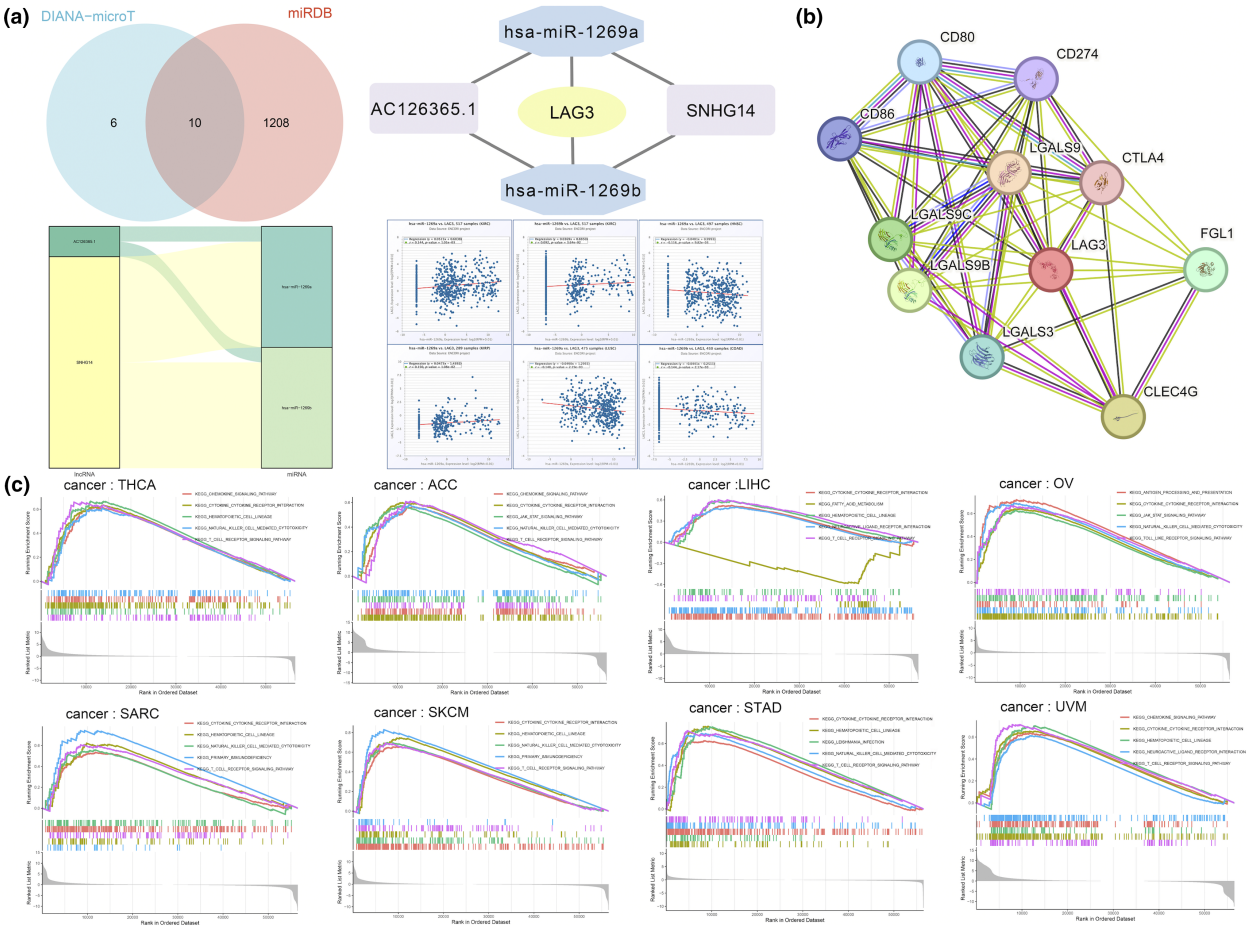

Figure 5. Regulation and function analysis of LAG3. **(a)** With DIANA-microT and miRDB databases, we performed an intersection and detected a total of 10 miRNAs. There were significant associations between hsa-miR-1269a expression and LAG3 expression in HNSC, KIRC, KIRP, LUSC, PAAD and TGCT ($P < 0.05$). The presence of hsa-miR-1269b also significantly influenced the expression of LAG3 in BRCA, COAD, KIRC and HNSC ($P < 0.05$). Hsa-miR-1269a and hsa-miR-1269b directly affected LAG3 expression and lncRNA AC126365.1 and SNHG14 indirectly regulated LAG3 expression by interacting with these two miRNAs. **(b)** LAG3 protein had close interactions with CD80, CD86, CD274, LGALS9, LGALS9B, LGALS9C, CTLA4, LGALS3, FGL1 and CLEC4G. **(c)** Signalling pathway analysis of LAG3. BRCA, breast cancer; COAD, colon adenocarcinoma; HNSC, head and neck squamous cell carcinoma; KIRC, kidney renal clear cell carcinoma; KIRP, kidney renal papillary cell carcinoma; LAG3, lymphocyte activation gene 3; lncRNA, long noncoding RNA; LUSC, lung squamous cell carcinoma; PAAD, pancreatic adenocarcinoma; TGCT, testicular germ cell tumours.

The genomic and proteomic networks of LAG3 at pan-cancer level

Next, we delved into the regulation and interplay of LAG3 at the transcriptional and translational levels. Using DIANA-microT and miRDB databases, we identified 16 and 1218 miRNAs, respectively, which were strongly related to LAG3. Then we performed an intersection and detected a total of 10 miRNAs, including hsa-miR-1269a and hsa-miR-1269b. There were significant associations between hsa-miR-1269a expression and LAG3 gene expression in HNSC, KIRC, KIRP, LUSC and TGCT ($P < 0.05$, Figure 5a, Supplementary figure 13a). Similarly, the presence of hsa-miR-1269b also significantly influenced the expression of LAG3 in BRCA, COAD, KIRC and HNSC ($P < 0.05$, Figure 5a, Supplementary figure 13a). Then, we constructed the competing endogenous RNA network of LAG3. Hsa-miR-1269a and hsa-miR-1269b directly affected LAG3 gene expression, and lncRNA AC126365.1 and SNHG14 indirectly regulated LAG3 gene expression by interacting with these two miRNAs (Figure 5a). We also

demonstrate PPI of LAG3 in Figure 5b. LAG3 protein had close interactions with CD80, CD86, CD274, LGALS9, LGALS9B, LGALS9C, CTLA4, LGALS3, FGL1 and CLEC4G.

Gene set enrichment analysis and mutation analysis

Figure 5c and Supplementary figure 13b intuitively demonstrate the results of the GSEA, revealing the five signalling pathways that were most significantly influenced by the expression of the LAG3 gene. We found that the TCR signalling pathway was significantly upregulated in ACC, CESC, LIHC, SARC, SKCM, STAD, THCA and UVM. The NK cell-mediated cytotoxicity pathway was enhanced in ACC, HNSC, OV, SARC, SKCM, STAD, THCA and TGCT. The primary immunodeficiency pathway was reinforced in CESC, HNSC, SARC and SKCM. The antigen processing and presentation pathway was enhanced in HNSC, OV and TGCT. The chemokine signalling pathway was upregulated in ACC, BLCA, THCA and UVM. The haematopoietic cell lineage pathway was enhanced in BLCA, LIHC, SARC, SKCM, STAD, THCA and UVM. These results indicated the complex effects of LAG3 on immunity in cancers.

Based on the data from the cBioPortal database, there was a high occurrence of amplification and mutation in the LAG3 gene across different forms of cancer (Figure 6a). The majority of mutations was missense mutations, with the most prevalent single nucleotide variation being cytosine. Regarding copy number variants (CNV), both heterozygous and homozygous amplification occurred in various cancer types (Supplementary figure 13c). The methylation and CNV levels of LAG3 in different cancer types and their influence on survival are shown in Supplementary figure 13d, e.

Correlations between LAG3 gene expression and tumour mutation were also analysed. Tumour mutation burden (TMB) and microsatellite instability (MSI) were substantiated to be associated with immunotherapy efficacy, and generally higher TMB and MSI values were associated with more benefits in immune-checkpoint inhibitor (ICI) therapy.[15–17] TMB and MSI values in 33 cancer types were utilised to reflect tumour mutation. The results are shown in the radar chart in Figure 6b. The correlation analysis showed that TMB values significantly increased with LAG3 gene expression in BRCA, COAD, GBM, LUAD, PRAD, THCA and UCEC. Conversely, in KIRP, mesothelioma, OV and TGCT, TMB values demonstrated negative correlations with LAG3 level ($P < 0.05$). For MSI, high LAG3 gene expression showed significant positive correlations in BLCA, BRCA, CESC, COAD, KIRC, LAML, LGG, LUAD, STAD, THYM and UCEC, while exhibiting negative correlations in KIRP, PRAD, TGCT and THCA ($P < 0.05$). In summary, the LAG3 gene had a high mutation rate in tumours and may serve as a potential target for immunotherapy.

Immunotherapy sensitivity analysis

The GDSC and CTRP databases were employed to uncover the correlation between LAG3 gene expression and drug sensitivity. In the GDSC database, LAG3 gene expression was positively related to the efficacy of 5-Fluorouracil, AZD8055, CAL-101, Navitoclax, VNLG/124 and Vorinostat ($P < 0.05$, Figure 6c). In the CTRP database, positive correlations between LAG3 gene expression and drug sensitivity were shown in CCT036477, cerulenin, LY-2183240, manumycin A, piperlongumine, PL-DI, PX-12 and PRIMA-1 ($P < 0.05$, Figure 6c).

In the CellMiner database (Figure 6d), LAG3 gene expression was positively correlated with the efficacy of fludarabine ($r = 0.380$, $P = 0.003$), OUABAIN ($r = 0.375$, $P = 0.003$), cladribine ($r = 0.372$, $P = 0.003$), ancitabine hydrochloride ($r = 0.432$, $P < 0.001$), gemcitabine ($r = 0.429$, $P < 0.001$), methylprednisolone ($r = 0.396$, $P = 0.002$) and cytarabine ($r = 0.381$, $P = 0.003$). More results are presented in Supplementary figure 14a, b.

DISCUSSION

LAG3 consists of four extracellular IgSF-like domains (D1-D4) and two intracellular regions, repetitive EP motif and KIEELE motif.[3,5] It is mainly expressed in activated T cells and NK cells, fulfilling a function of immunosuppression.[13] In this study, we revealed the prognostic effect of LAG3 in renal cancers using IHC staining and statistical analyses. We also explored the differential expression and biological characteristics of LAG3, along with its impact on survival, the tumour microenvironment and the efficacy of immunotherapy at pan-caner level.

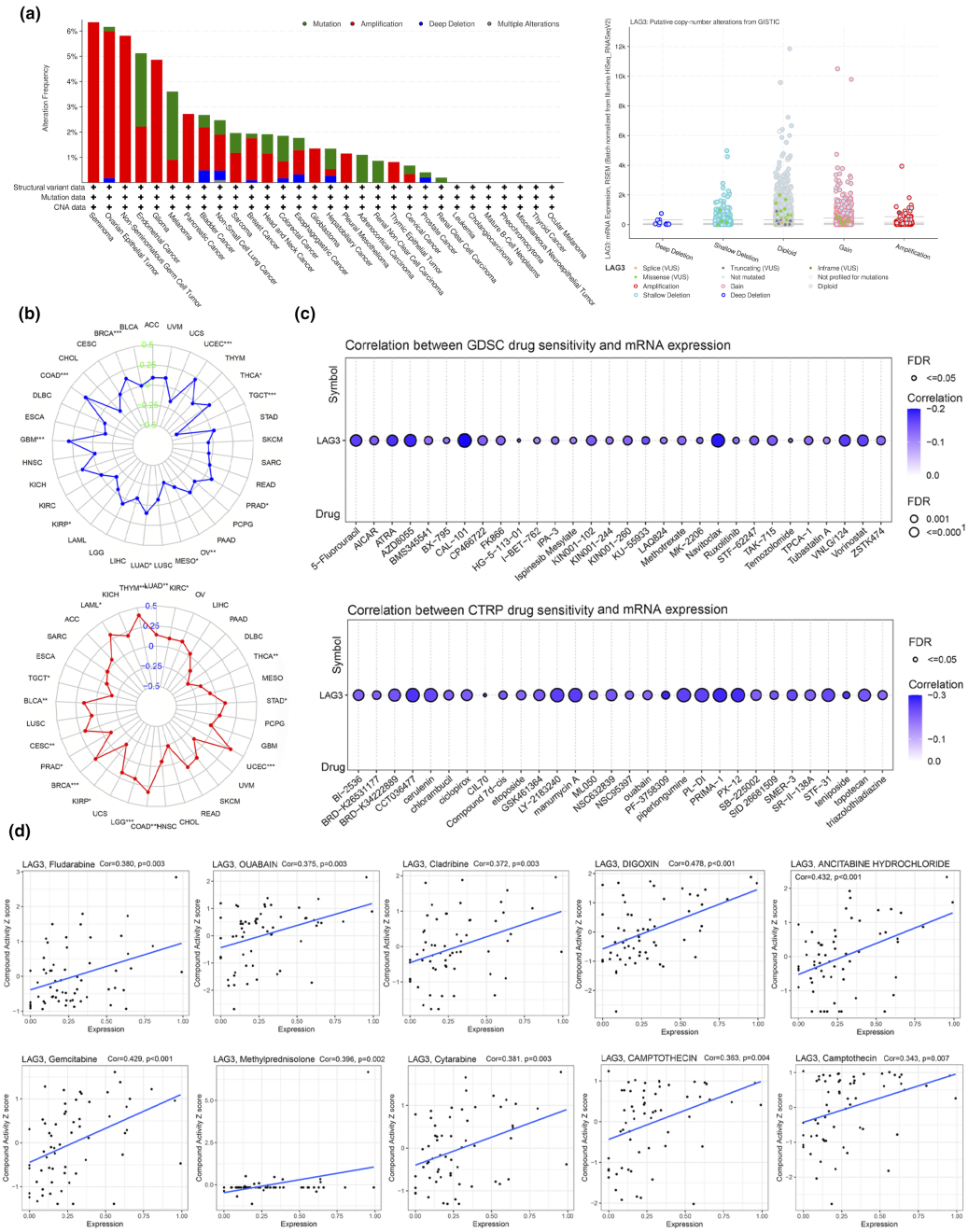

Figure 6. Mutation of LAG3 and drug sensitivity. **(a)** There was a high occurrence of amplification and mutation in the LAG3 gene across different forms of cancer. **(b)** TMB values significantly increased with LAG3 expression in BRCA, COAD, GBM, LUAD, PRAD, THCA and UCEC. Conversely, in KIRP, MESO, OV and TGCT, TMB values demonstrated negative correlations with LAG3 levels ($P < 0.05$). For MSI, high LAG3 expression showed significant positive correlations in BLCA, BRCA, CESC, COAD, KIRC, LAML, LGG, LUAD, STAD, THYM and UCEC, while exhibiting negative correlations in KIRP, PRAD, TGCT and THCA ($P < 0.05$). **(c, d)** Drug sensitivity analyses in GDSC, CTRP and CellMiner databases. BLCA, bladder urothelial carcinoma; BRCA, breast cancer; CESC, cervical squamous cell carcinoma and endocervical adenocarcinoma; COAD, colon adenocarcinoma; CTRP, cancer therapy response portal; GBM, glioblastoma multiforme; GDSC, genomics of drug sensitivity in cancer; KIRC, kidney renal clear cell carcinoma; KIRP, kidney renal papillary cell carcinoma; LAG3, lymphocyte activation gene 3; LAML, acute myeloid leukaemia; LGG, lower grade glioma; LUAD, lung adenocarcinoma; MESO, mesothelioma; MSI, microsatellite instability; OV, ovarian serous cystadenocarcinoma; PRAD, prostate adenocarcinoma; STAD, stomach adenocarcinoma; TGCT, testicular germ cell tumours; THCA, thyroid carcinoma; THYM, thymoma; TMB, tumour mutation burden; UCEC, uterine corpus endometrial carcinoma; $^{*}P < 0.05$; $^{**}P < 0.01$; $^{***}P < 0.001$.

LAG3 was a pivotal biomarker in tumour prognosis

Initially, through IHC staining and differential analysis, we demonstrated significant differences in LAG3 gene expression between tumour and normal tissues. Our results illustrated that LAG3 protein expression was significantly higher in normal tissue compared to tumour tissue. The underlying reasons for this phenomenon have not been fully elucidated. In previous studies, Klümper *et al*.[18] found that the methylation status of the LAG3 promoter negatively correlated with levels of LAG3 messenger RNA expression in patients with renal cell carcinoma. Consequently, excessive methylation of the LAG3 promoter may be present in renal cancer tissues from the Xinhua cohort. Further validation was needed to clarify the reasons underlying the dynamic changes in LAG3 expression. Then, we performed a comprehensive clinical analysis to investigate the influence of LAG3 gene expression on survival and tumour stage, as well as its correlation with other clinical variables. We identified high LAG3 gene expression as an independent unfavourable prognostic factor for OS (HR = 6.60, 95% CI = 2.43–17.90, $P < 0.001$) and PFS (HR = 3.44, 95% CI = 1.68–7.10, $P < 0.001$). Then, at the pan-cancer level, LAG3 gene expression also indicated significantly shorter OS, PFS and DSS in LGG (HR = 1.636, 1.336, 1.630 respectively), THYM (HR = 2.104, 1.499, 3.163 respectively) and UVM (HR = 1.496, 1.310, 1.450 respectively), while higher in BLCA (HR = 0.866, 0.849, 0.817 respectively), CESC (HR = 0.695, 0.690, 0.640 respectively) and SKCM (HR = 0.788, 0.899, 0.753 respectively). Additionally, correlations between LAG3 gene expression and tumour prognosis were also reported in a few studies. Hu *et al*.[19] reported that the infiltration of $LAG3^+$ lymphocytes ameliorated OS in patients with triple-negative breast cancer. Peng *et al*.[20] discovered a positive correlation between LAG3 gene expression and better SKCM prognosis. These results confirmed the intricate yet important role of LAG3 gene expression in prognosis. The detrimental effects may come from T-cell exhaustion caused by LAG3, leading to a cessation of cytokine production and a progressive and hierarchical loss of effector functions.[21–24] The protective effect may arise from the high infiltration and hyperactivation of the immune system mediated by LAG3.[25,26] Combined with the differential expression between normal and tumour, as well as prognostic analyses, we proposed that LAG3 was an independent prognostic biomarker for kidney neoplasm and had a considerable impact on the prognosis in multiple cancer types, especially BLCA, CESC, SKCM and UVM.

LAG3 was strongly associated with immunity and indicated a highly infiltrated but dysfunctional TIME, playing an immunosuppressive role

TIME exerts an essential effect on tumour immune surveillance and the efficacy of immunotherapy.[27–29] Our research showed that in cases of kidney neoplasm, LGG, UVM and THYM, increased LAG3 gene expression was correlated with more immune cell infiltration and stromal components. To be specific, the infiltration of activated NK cells, plasma cells, Tregs, Tfhs, macrophages M1 and $CD8^+$ T cells rose, while resting memory T cells, resting NK cells and macrophage M2 dropped. Thus, we concluded that there was a strong correlation between elevated LAG3 gene expression and increased immune score or stromal score in many cancers. Specifically, high LAG3 gene expression was associated with increased infiltration of effective or activated T cells and decreased infiltration of resting lymphocytes along with NK cells and macrophages M1. Combined with the negative prognosis in these cancers, we proposed a potential hypothesis that LAG3 presence may elevate immune infiltration and subsequently exhaust the infiltrated immune cells. This theory was further corroborated by the TIDE database. Results showed that LAG3 gene expression was positively correlated with CTL infiltration and dysfunction scores, leading to a bad prognosis.

In addition, the biological function of LAG3 also contributed to the explanation of this theory. LAG3 would cause T-cell suppression and exhaustion and facilitate tumour progression, resulting in the release of immune factors[30–32] and the recruitment of more T cells in TIME.[33] The immunosuppressive effect of LAG3 on T cells is initiated by the binding of LAG3 to its ligands. As demonstrated in Figure 5b, in addition to MHC class II, which serves as a prototypical ligand for LAG3, several other prominent immunosuppressive ligands include fibrinogen-like

protein 1 (FGL-1), C-type lectin domain family 4 member G and Galectin-3 (LGALS3). FGL-1 is overexpressed in cancer cells, and its interaction with LAG3 inhibits antigen-specific T-cell responses, thereby promoting immune evasion and resistance to immunotherapy. LSECtin, commonly expressed in melanomas, interacts with LAG3 to blunt tumour-specific T-cell responses by downregulating cell cycle kinases. Additionally, LGALS3, a 31-kDa lectin, binds to LAG3 and mediates the suppression of $CD8^+$ T cells. In our research and previous studies, we also revealed a correlation between LAG3 gene expression and the upregulation of chemokines. And this upregulation was associated with a heightened influx of immune cells.[30,34,35] Furthermore, we also noticed a higher expression of LAG3 in $CXCL13^+$ TfhTh1, $CXCL13^+$ Tex and $PDCD1^+$ Tex. CXCL13, in conjunction with CXCR5, could exert a potent chemotactic effect on B cells while also exerting a mild chemoattractant effect on $CXCR5^+$ T cells and macrophages.[36,37] The CXCL13/CXCR5 axis is linked with the progression of several cancer types and is regarded as a biomarker of T-cell exhaustion.[38,39] Research has emphasised the crucial role of CXCL13 in the maintenance of the antitumor microenvironment (through $CXCR5^+CD8^+$ T cells) and its biomarker use in the evaluation of ICI efficacy.[40,41] PDCD1, known for programming PD-1, is responsible for inducing immunosuppression and immune evasion. Higher LAG3 gene expression on $PDCD1^+$ Tex indicated a close correlation between LAG3 and other immunosuppressive factors.[42]

In general, LAG3 exhibited a robust association with other immune-related molecules, resulting in a combined immunosuppressive effect. Furthermore, it would cause a high-infiltration but low-function TIME in many types of cancer.

LAG3 was a promising biomarker in immunotherapy

ICI therapy is considered one of the most promising immunotherapies in cancer treatments, and LAG3 is believed to make a magnificent contribution.[12,43] This study provided evidence for a strong correlation between LAG3 gene expression and TMB as well as MSI in many cancers (KIRC, KIRP, CESC and LGG in MSI; KIRP, BRCA and COAD in TMB). These findings suggested potential advantages for patients receiving ICI therapies.[15–17] Besides, LAG3 gene expression was also associated with low tumour purity in kidney neoplasm, UVM, THYM and LGG, which was expected to connect with improved responses to immunotherapy.[44] Previous studies also confirmed LAG3 as a promising target for immunotherapy.[44–47] Certain specific medicines, for instance, MK-280[48] or MGD013,[49] were validated to be effective. In addition, the aforementioned findings (LAG3 gene expression was correlated with multiple immune-related genes) also suggested a potential effectiveness in co-blockage of LAG3 and other immune targets. For instance, Zelba *et al.*[50] identified a co-expression relationship between LAG3 and PD-1 in renal cell carcinoma, while Liu *et al.*[51] demonstrated a co-expression relationship between LAG3 and CTLA-4 in breast cancer. Combinatorial anti-LAG3 and anti-PD-1 therapy has also demonstrated benefits for patients resistant to primary anti-PD-1 and PD-L1 therapy.[14] Moreover, a bispecific antibody that targets both LAG3 and PD-L1 has been shown to enhance effector T-cell responses and exhibit antitumor efficacy in humanised xenograft models.[52] Therefore, LAG3 was a promising biomarker in immunotherapy and can subsequently play an essential role in prognosis.

Limitations

Our investigation has certain limitations. Initially, a total of 370 patients were enrolled only in Xinhua Hospital, which might slightly affect the validity of the conclusion. In addition, our pan-cancer investigation was conducted using several public databases, primarily consisting of data from patients in the Western countries. This might introduce potential racial disparities in our study. Our research emphasises uncovering the role of LAG3 as a biomarker throughout the entire tumour microenvironment, rather than being confined to a specific immune cell population. The role of LAG3 expression specifically in these cells remained unknown. Further research will be undertaken to investigate the dynamic changes in LAG3 expression on T cells and NK cells throughout tumour progression. Last but not least, though we have shown the correlation between LAG3 gene expression and prognosis, tumour characteristics, immune functions and immunotherapy at the pan-cancer level, more detailed and complex molecular functions of LAG3 for each type of cancer remain to be elucidated in the future.

CONCLUSION

Our study identified LAG3 as an independent unfavourable factor for both OS (HR = 6.60, 95% CI = 2.43–17.90, $P < 0.001$) and PFS (HR = 3.44, 95% CI = 1.68–7.10, $P < 0.001$) in kidney neoplasm. Furthermore, pan-cancer analysis also revealed LAG3 gene expression to be a potent prognostic biomarker in other malignancies, such as BLCA, LGG and UVM. Moreover, LAG3 served as a biomarker for the TIME, which featured high infiltration but low function. Finally, we constructed the ceRNAs and PPI networks, demonstrated the strong relationship between LAG3 and immunity and predicted drug sensitivities related to LAG3.

METHODS

Patient eligibility in our study

The study, with ethical approval granted by the ethics committee of Xinhua Hospital affiliated with Shanghai Jiao Tong University School of Medicine (XHEC-C-2021-145-1), encompassed individuals diagnosed with kidney neoplasms who underwent curative surgery at our institution from 2016 to 2018. Specifically, inclusion criteria mandated the availability of tumour tissue sections for research purposes, resulting in a cohort of 370 patients meeting these criteria. Due to inadequate IHC staining information, the tumour tissues from two patients and the normal tissues from 64 patients were removed. Moreover, 75 people were disqualified from the chi-square test and Kaplan–Meier survival analysis because OS and PFS, two important follow-up variables, were lacking. Furthermore, due to limited data, we were unable to evaluate the relevant link between OS censoring and progression data for 71 individuals and LAG3 protein expression. Moreover, 16 individuals were excluded from the multivariate Cox regression analysis since their histological classifications were assigned as 'Others.' The follow-up period ended up in March 2021. OS was delineated as the duration from the initial diagnosis of kidney neoplasm to either the date of death or the last recorded follow-up. Similarly, PFS was defined as the duration between the initiation of treatment and the occurrence of progression, death, or the last follow-up. Finally, demographic factors, tumour characteristics, follow-up details and IHC staining information are presented through a heatmap and a table.

Immunohistochemical staining

The tumour tissue and adjacent normal tissue of patients were initially fixed, embedded and sectioned into paraffin samples post-surgery. Afterwards, the samples were dewaxed and rehydrated, followed by antigen retrieval to expose the antigen LAG3, utilising citric acid (pH = 6.0) antigen-retrieval buffers. To minimise non-antibody binding, the samples underwent incubation in a 3% hydrogen peroxide solution, followed by subsequent washing in phosphate-buffered saline solution. Next, to block endogenous peroxidase activity, the samples were subjected to treatment with 3% bovine serum albumin. Afterwards, primary antibodies (Proteintech, Wuhan, China, 29 548-1-AP, 1:200) were utilised for specific binding, followed by the introduction of secondary antibodies labelled with HRP enzyme. The secondary antibodies selectively bound to the primary antibodies, facilitating the formation of a detection complex. Then, the specific substrate introduced for HRP was DAB, initiating a chromogenic reaction. In the presence of the target antigens, DAB reacted with HRP, leading to a visually detectable colour change. Moreover, to enhance visualisation, haematoxylin was added as a counterstain, providing contrast and highlighting the nuclei and the samples then underwent dehydration using a series of graded alcohols. Finally, all slides were examined under a light microscope, and two professional pathologists were enlisted to read and score these slides. When the opinions of the two pathologists conflicted, the third pathologist would carefully check and determine the final results.

Scoring the immunohistochemical staining

The scoring of IHC staining was conducted according to the following criteria, enabling the quantification of LAG3 protein expression levels in tissue slides. Since LAG3 is predominantly localised to the cell membrane, the IHC staining scores were assessed based on membrane-positive staining. Scoring involved two key factors: staining intensity and the extent of the stained area. Intensity categories included negative, weak positive, positive and strong positive, scored as 0, 1, 2 and 3 respectively. The stained area was classified into four categories: $< 10\%$, 10–39%, 40–69% and 70–100%, corresponding to scores of 1, 2, 3 and 4. Following this, the scores for both tumour and normal tissues were obtained by multiplying the intensity and area scores. Finally, the scores for tumour tissue were categorised into two groups: low (0–8) and high (9–12).

Exploring the relationship between LAG3 gene expression level and clinical variables

First, Wilcoxon tests compared LAG3 scores between tumour and normal tissues, visualised with a violin plot. A K-M survival analysis was conducted to explore the correlation between LAG3 gene expression levels and OS/PFS. The optimal cut-off for LAG3 gene expression was determined using the 'surv_cutpoint' and 'surv_categorize' functions of an R package, categorising patients into two groups to maximise differences in OS/PFS. Subsequent to this, Pearson Chi-square tests were utilised to identify associations between categorical variables and the two LAG3 groups, with significance marked by asterisks: '*' ($P < 0.05$), '**' ($P < 0.01$) and '***' ($P < 0.001$). Then, a multivariate Cox regression analysis was performed to assess whether LAG3 gene expression levels independently influenced OS or PFS. To be precise, patients with histopathological classifications other than KIRC, KIRP and

KICH were excluded from the analysis. The risk score was calculated from the Cox model as follows:

$$\text{Risk Score} = \beta_1 \times \text{Variable}_1 + \beta_2 \times \text{Variable}_2 + \ldots + \beta_n \times \text{Variable}_n.$$

Each variable's coefficient (β) was derived from the Cox model. Patients were stratified by the median risk score, and a K-M survival analysis was performed. Finally, Chi-square tests examined associations between clinical stages and risk score-based groups.

Validation of the models and construction of nomograms

To validate our regression analysis for OS and PFS, we presented residual plots and determined the concordance index (C-index). Next, Schoenfeld global and individual tests were also performed to assess the proportional hazards assumption. The global test evaluated whether the assumption held across the entire model, while the individual tests assessed each covariate separately. Following this, for ease of prediction, nomograms were developed utilising the variables in the Cox model to forecast survival or progression-free probabilities for 1, 2, 3, 4 and 5 years. We selected six variables from three different perspectives: demographic (age category and gender), tumour characteristics (histopathological classification, Fuhrman nuclear stage and tumour stage, which were validated as significant prognostic factors[53]), and the impact of LAG3 (LAG3 classification), to include in our regression models. We constructed a nomogram based on this regression model. It should be noted that higher total scores meant a low probability of survival in the nomogram. And a higher nomogram score for the curtain variable indicated that the variable had a more negative impact on prognosis. Lastly, calibration and discrimination performances were assessed through calibration curves and receiver operating characteristic curves.

Data collection for our bioinformatics analysis

The gene expression profiles of LAG3 for 11 057 samples among 33 cancer types were downloaded from the TCGA database (https://cancergenome.nih.gov/).[54] Also, demographic factors and survival indicators such as OS, PFS, DFS and DSS were extracted. Moreover, tumour characteristics such as clinical stages, the ESTIMATE score, TMB and MSI were downloaded from the TCGA database for subsequent statistical analyses. Furthermore, through gene expression profile assessment, CIBERSORT was applied to calculate the degree of immune infiltration and the fraction of distinct immune cell subtypes. The distribution pattern and expression levels of LAG3 in subtypes of myeloid cells, T cells and NK cells were obtained by downloading data from the SCDVA databases (http://panmyeloid.cancer-pku.cn/, http://pan-nk.cancer-pku.cn/) and the ScRNA-seq Data Portal for T cells in the Pan-Cancer database (http://cancer-pku.cn:3838/PanC_T/).[55–57] Additionally, we employed the TIMER 2.0 database (http://timer.cistrome.org/) and the TIDE database. Information regarding the correlation between LAG3 and immune cell infiltration as well as the association between LAG3 and immunotherapy was downloaded from these databases. Using data in DIANA-microT (https://dianalab.e-ce.uth.gr/microt_webserver/#/) and miRDB (https://mirdb.org/) databases, we constructed the competing endogenous RNA network. Then the protein–protein interaction of LAG3 was also downloaded in the String database (https://cn.string-db.org/). Subsequently, we utilised the cBioPortal (https://www.cbioportal.org/) and the Gene Set Cancer Analysis databases (http://bioinfo.life.hust.edu.cn/GSCA) to analyse the mutation and signalling pathway at the pan-cancer level. Drug sensitivity analysis employed CellMiner (https://discover.nci.nih.gov/cellminer/home.do), Cancer Therapy Response Portal (CTRP) (https://portals.broadinstitute.org/ctrp/) and Genomics of Drug Sensitivity in Cancer (GDSC) databases (https://www.cancerrxgene.org) to reveal the correlation between LAG3 and the efficacy of various drugs.

Data analysis processing

First, Wilcoxon tests were conducted across 33 tumour types to analyse the differential gene expression between tumour and normal tissues. Patients were then stratified into two groups using the median LAG3 gene expression, followed by K-M survival analysis for OS, PFS, DFS and DSS, with results presented only for $P < 0.05$. Following this, univariate Cox regression was used to calculate the HR of LAG3 for these survival metrics in all 33 TCGA tumour types. We also employed differential expression analysis across clinical stages among the 33 cancers. The ESTIMATE score was utilised to assess stromal and immune cell proportions within the tumour microenvironment. Following this, co-expression analysis was carried out with LAG3 gene expression.[58] In light of immune infiltration, we also conducted correlation analysis to examine the tumour microenvironment across these cancers. Pearson correlation analysis explored the association between LAG3 and 47 key immune-related genes. We further analysed LAG3 expression in myeloid cells, T cells and NK cells at the pan-cancer level and also examined its correlation with immune cell infiltration and T-cell functional states. Additionally, we constructed a competing endogenous RNA network, protein–protein interaction for LAG3, and performed GSEA to identify the top five significant pathways across cancers. Using the cBioPortal database, we analysed LAG3 mutations. We also explored the correlation between LAG3 expression and TMB/MSI, which are critical for predicting therapeutic efficacy across cancer types. Finally, we assessed the correlation between LAG3 expression and drug sensitivity.

Quantitative statistical analysis

In this research, results with both a false discovery rate and a two-tailed *P*-value <0.05 were determined to be statistically significant. Statistical processes were performed with R (Institute for Statistics and Mathematics, version 4.2.3; www.r-project.org; Vienna, Austria) and Python version 3.6 software (https://www.python.org/). Descriptive statistics used mean $\pm$ SD for normal distributed continuous

data and median with range for non-normally distributed continuous variables. Furthermore, parametric tests were used to compare means of various groups where variables followed a Gaussian distribution and had homogeneous variance. Otherwise, nonparametric tests were used. Parametric and nonparametric tests included the *t*-test, the Pearson correlation, the Wilcoxon test and the Spearman correlation.

ACKNOWLEDGMENTS

We thank TCGA database, STRING database, HPA database, cBioportal database, DIANA-microT database, miRWalk database, miRDB database, miRcode database, starbase, CellMiner database, GSVA database, SCDVA database, ScRNA-seq Data Portal for T cells in Pan-Cancer database, TIMER 2.0 database and TIDE database for allowing us to use their data. This work was sponsored by the National Natural Science Foundation of China (No. 82072806); Shanghai Rising-Star Program (23QC1401400); Shanghai Rising-Star Program (Sailing Special Program) (23YF1458400); Bole Project of Shanghai Jiao Tong University. The funders had no role in study design, data collection and analysis, decision to publish or preparation of the manuscript.

AUTHOR CONTRIBUTIONS

Yifan Liu: Conceptualization; formal analysis; writing – original draft. **Yuntao Yao:** Conceptualization; formal analysis; writing – original draft. **Xinyue Yang:** Conceptualization; writing – original draft. **Maodong Wei:** Conceptualization; writing – original draft. **Bingnan Lu:** Conceptualization; writing – review and editing. **Keqing Dong:** Data curation; writing – original draft. **Donghao Lyu:** Writing – original draft. **Yuanan Li:** Writing – original draft. **Wenbin Guan:** Writing – review and editing. **Runzhi Huang:** Conceptualization; formal analysis; writing – review and editing. **Guofeng Xu:** Writing – review and editing. **Xiuwu Pan:** Conceptualization; data curation; writing – review and editing.

CONFLICT OF INTEREST

The authors declare that there are no conflicts of interest.

DATA AVAILABILITY STATEMENT

The datasets generated and/or analysed during the current study are available on the Cancer Genome Atlas (TCGA) database (https://cancergenome.nih.gov/), the Search Tools for the Retrieval of Interacting Genes/Proteins (STRING) database (https://string-db.org/), cBioportal database (https://www.cbioportal.org/), DIANA-microT database (https://dianalab.e-ce.uth.gr/microt_webserver/#/), miRDB database (https://mirdb.org/), CellMiner database (https://discover.nci.nih.gov/cellminer/home.do), the Gene Set Cancer Analysis (GSCA) websites (http://bioinfo.life.hust.edu.cn/GSCA), Cancer Therapy Response Portal (CTRP) database (https://portals.broadinstitute.org/ctrp/), Genomics of Drug Sensitivity in Cancer (GDSC) database (https://www.cancerrxgene.org), ScRNA-seq Data Visualisation and Analysis (SCDVA) database (http://panmyeloid.cancer-pku.cn/, http://pan-nk.cancer-pku.cn/), ScRNA-seq Data Portal for T cell in Pan-Cancer database (http://cancer-pku.cn:3838/PanC_T/), Tumour Immune Estimation Resource (TIMER) 2.0 database (http://timer.cistrome.org/) and Tumour Immune Dysfunction and Exclusion (TIDE) database. Please contact the corresponding author for access to the data in this manuscript. We are more than pleased to share our data for further research under reasonable request.

ETHICS APPROVAL

The study was approved by the Ethics Committee of Xinhua Hospital Affiliated to Shanghai Jiao Tong University School of Medicine (XHEC-C-2021-145-1). All authors confirmed that all methods were carried out in accordance with relevant guidelines and regulations.

CONSENT

For our Xinhua cohort, consent was obtained from the participants (or from parents or legal guardians for children under 16). Any personally identifiable biomedical, clinical or biometric data included in the manuscript was obtained with informed consent from the subjects.

REFERENCES

1. Triebel F, Jitsukawa S, Baixeras E *et al*. LAG-3, a novel lymphocyte activation gene closely related to CD4. *J Exp Med* 1990; **171**: 1393–1405.
2. Hannier S, Triebel F. The MHC class II ligand lymphocyte activation gene-3 is co-distributed with CD8 and CD3-TCR molecules after their engagement by mAb or peptide-MHC class I complexes. *Int Immunol* 1999; **11**: 1745–1752.
3. Huard B, Mastrangeli R, Prigent P *et al*. Characterization of the major histocompatibility complex class II binding site on LAG-3 protein. *Proc Natl Acad Sci USA* 1997; **94**: 5744–5749.
4. Wang JH, Meijers R, Xiong Y *et al*. Crystal structure of the human CD4 N-terminal two-domain fragment complexed to a class II MHC molecule. *Proc Natl Acad Sci USA* 2001; **98**: 10799–10804.
5. Mastrangeli R, Micangeli E, Donini S. Cloning of murine LAG-3 by magnetic bead bound homologous probes and PCR (gene-capture PCR). *Anal Biochem* 1996; **241**: 93–102.
6. Durante MA, Rodriguez DA, Kurtenbach S *et al*. Single-cell analysis reveals new evolutionary complexity in uveal melanoma. *Nat Commun* 2020; **11**: 496.
7. Arimura K, Hiroshima K, Nagashima Y *et al*. LAG3 is an independent prognostic biomarker and potential target for immune checkpoint inhibitors in malignant pleural mesothelioma: a retrospective study. *BMC Cancer* 2023; **23**: 1206.
8. Shi AP, Tang XY, Xiong YL *et al*. Immune checkpoint LAG3 and its ligand FGL1 in cancer. *Front Immunol* 2021; **12**: 785091.

9. Wang J, Sanmamed MF, Datar I *et al*. Fibrinogen-like protein 1 is a major immune inhibitory ligand of LAG-3. *Cell* 2019; **176**: 334–347.e312.
10. Huang CT, Workman CJ, Flies D *et al*. Role of LAG-3 in regulatory T cells. *Immunity* 2004; **21**: 503–513.
11. Lu B, Liu Y, Yao Y *et al*. Unveiling the unique role of TSPAN7 across tumors: a pan-cancer study incorporating retrospective clinical research and bioinformatic analysis. *Biol Direct* 2024; **19**: 72.
12. Aggarwal V, Workman CJ, Vignali DAA. LAG-3 as the third checkpoint inhibitor. *Nat Immunol* 2023; **24**: 1415–1422.
13. Andrews LP, Marciscano AE, Drake CG, Vignali DA. LAG3 (CD223) as a cancer immunotherapy target. *Immunol Rev* 2017; **276**: 80–96.
14. Ascierto PA, Lipson EJ, Dummer R *et al*. Nivolumab and Relatlimab in patients with advanced melanoma that had progressed on anti-programmed Death-1/programmed death ligand 1 therapy: results from the phase I/IIa RELATIVITY-020 trial. *J Clin Oncol* 2023; **41**: 2724–2735.
15. Chan TA, Yarchoan M, Jaffee E *et al*. Development of tumor mutation burden as an immunotherapy biomarker: utility for the oncology clinic. *Ann Oncol* 2019; **30**: 44–56.
16. Hou W, Yi C, Zhu H. Predictive biomarkers of colon cancer immunotherapy: present and future. *Front Immunol* 2022; **13**: 1032314.
17. Li K, Luo H, Huang L, Luo H, Zhu X. Microsatellite instability: a review of what the oncologist should know. *Cancer Cell Int* 2020; **20**: 16.
18. Klümper N, Ralser DJ, Bawden EG *et al*. LAG3 (LAG-3, CD223) DNA methylation correlates with LAG3 expression by tumor and immune cells, immune cell infiltration, and overall survival in clear cell renal cell carcinoma. *J Immunother Cancer* 2020; **8**: e000552.
19. Hu G, Wang S, Wang S, Ding Q, Huang L. LAG-3$^+$ tumor-infiltrating lymphocytes ameliorates overall survival in triple-negative breast cancer patients. *Front Oncol* 2022; **12**: 986903.
20. Peng J, Du Z, Sun Y, Zhou Z. A combined analysis of multi-omics data reveals the prognostic values and immunotherapy response of LAG3 in human cancers. *Eur J Med Res* 2023; **28**: 604.
21. Zajac AJ, Blattman JN, Murali-Krishna K *et al*. Viral immune evasion due to persistence of activated T cells without effector function. *J Exp Med* 1998; **188**: 2205–2213.
22. Wherry EJ. T cell exhaustion. *Nat Immunol* 2011; **12**: 492–499.
23. Doering TA, Crawford A, Angelosanto JM, Paley MA, Ziegler CG, Wherry EJ. Network analysis reveals centrally connected genes and pathways involved in CD8$^+$ T cell exhaustion versus memory. *Immunity* 2012; **37**: 1130–1144.
24. Schietinger A, Greenberg PD. Tolerance and exhaustion: defining mechanisms of T cell dysfunction. *Trends Immunol* 2014; **35**: 51–60.
25. Workman CJ, Dugger KJ, Vignali DA. Cutting edge: molecular analysis of the negative regulatory function of lymphocyte activation gene-3. *J Immunol* 2002; **169**: 5392–5395.
26. Chocarro L, Blanco E, Zuazo M *et al*. Understanding LAG-3 signaling. *Int J Mol Sci* 2021; **22**: 5282.
27. Zhang Y, Chen L. Classification of advanced human cancers based on tumor immunity in the MicroEnvironment (TIME) for cancer immunotherapy. *JAMA Oncol* 2016; **2**: 1403–1404.
28. Nagarsheth N, Wicha MS, Zou W. Chemokines in the cancer microenvironment and their relevance in cancer immunotherapy. *Nat Rev Immunol* 2017; **17**: 559–572.
29. Binnewies M, Roberts EW, Kersten K *et al*. Understanding the tumor immune microenvironment (TIME) for effective therapy. *Nat Med* 2018; **24**: 541–550.
30. Gorbachev AV, Fairchild RL. Regulation of chemokine expression in the tumor microenvironment. *Crit Rev Immunol* 2014; **34**: 103–120.
31. Rot A, von Andrian UH. Chemokines in innate and adaptive host defense: basic chemokinese grammar for immune cells. *Annu Rev Immunol* 2004; **22**: 891–928.
32. Mantovani A. The chemokine system: redundancy for robust outputs. *Immunol Today* 1999; **20**: 254–257.
33. Ozga AJ, Chow MT, Luster AD. Chemokines and the immune response to cancer. *Immunity* 2021; **54**: 859–874.
34. Reschke R, Gajewski TF. CXCL9 and CXCL10 bring the heat to tumors. *Sci Immunol* 2022; **7**: eabq6509.
35. Hoch T, Schulz D, Eling N, Gómez JM, Levesque MP, Bodenmiller B. Multiplexed imaging mass cytometry of the chemokine milieus in melanoma characterizes features of the response to immunotherapy. *Sci Immunol* 2022; **7**: eabk1692.
36. Gunn MD, Ngo VN, Ansel KM, Ekland EH, Cyster JG, Williams LT. A B-cell-homing chemokine made in lymphoid follicles activates Burkitt's lymphoma receptor-1. *Nature* 1998; **391**: 799–803.
37. Sáez de Guinoa J, Barrio L, Mellado M, Carrasco YR. CXCL13/CXCR5 signaling enhances BCR-triggered B-cell activation by shaping cell dynamics. *Blood* 2011; **118**: 1560–1569.
38. Li H, van der Leun AM, Yofe I *et al*. Dysfunctional CD8 T cells form a proliferative, dynamically regulated compartment within human melanoma. *Cell* 2019; **176**: 775–789.e718.
39. Hussain M, Adah D, Tariq M, Lu Y, Zhang J, Liu J. CXCL13/CXCR5 signaling axis in cancer. *Life Sci* 2019; **227**: 175–186.
40. Yang M, Lu J, Zhang G *et al*. CXCL13 shapes immunoactive tumor microenvironment and enhances the efficacy of PD-1 checkpoint blockade in high-grade serous ovarian cancer. *J Immunother Cancer* 2021; **9**: e001136.
41. Liu B, Zhang Y, Wang D, Hu X, Zhang Z. Single-cell meta-analyses reveal responses of tumor-reactive CXCL13$^+$ T cells to immune-checkpoint blockade. *Nat Cancer* 2022; **3**: 1123–1136.
42. Pardoll DM. The blockade of immune checkpoints in cancer immunotherapy. *Nat Rev Cancer* 2012; **12**: 252–264.
43. Ruffo E, Wu RC, Bruno TC, Workman CJ, Vignali DAA. Lymphocyte-activation gene 3 (LAG3): the next immune checkpoint receptor. *Semin Immunol* 2019; **42**: 101305.
44. Gong Z, Zhang J, Guo W. Tumor purity as a prognosis and immunotherapy relevant feature in gastric cancer. *Cancer Med* 2020; **9**: 9052–9063.
45. Mao Y, Feng Q, Zheng P *et al*. Low tumor purity is associated with poor prognosis, heavy mutation burden, and intense immune phenotype in colon cancer. *Cancer Manag Res* 2018; **10**: 3569–3577.

46. Qi X, Qi C, Qin B, Kang X, Hu Y, Han W. Immune-stromal score signature: novel prognostic tool of the tumor microenvironment in lung adenocarcinoma. *Front Oncol* 2020; **10**: 541330.
47. Deng Y, Song Z, Huang L *et al*. Tumor purity as a prognosis and immunotherapy relevant feature in cervical cancer. *Aging (Albany NY)* 2021; **13**: 24768–24785.
48. Bhagwat B, Cherwinski H, Sathe M *et al*. Establishment of engineered cell-based assays mediating LAG3 and PD1 immune suppression enables potency measurement of blocking antibodies and assessment of signal transduction. *J Immunol Methods* 2018; **456**: 7–14.
49. LaMotte-Mohs R, Shah K, Smith D *et al*. MGD013, a bispecific PD-1 x LAG-3 dual-affinity re-targeting (DART®) protein with T-cell immunomodulatory activity for cancer treatment. *Cancer Res* 2016; **76**(14 Suppl): 3217.
50. Zelba H, Bedke J, Hennenlotter J *et al*. PD-1 and LAG-3 dominate checkpoint receptor-mediated T-cell inhibition in renal cell carcinoma. *Cancer Immunol Res* 2019; **7**: 1891–1899.
51. Liu Q, Qi Y, Zhai J *et al*. Molecular and clinical characterization of LAG3 in breast cancer through 2994 samples. *Front Immunol* 2021; **12**: 599207.
52. Sung E, Ko M, Won JY *et al*. LAG-3xPD-L1 bispecific antibody potentiates antitumor responses of T cells through dendritic cell activation. *Mol Ther* 2022; **30**: 2800–2816.
53. Klatte T, Rossi SH, Stewart GD. Prognostic factors and prognostic models for renal cell carcinoma: a literature review. *World J Urol* 2018; **36**: 1943–1952.
54. Tomczak K, Czerwinska P, Wiznerowicz M. The cancer genome atlas (TCGA): an immeasurable source of knowledge. *Contemp Oncol (Pozn)* 2015; **19**: A68–A77.
55. Cheng S, Li Z, Gao R *et al*. A pan-cancer single-cell transcriptional atlas of tumor infiltrating myeloid cells. *Cell* 2021; **184**: 792–809.e723.
56. Zheng L, Qin S, Si W *et al*. Pan-cancer single-cell landscape of tumor-infiltrating T cells. *Science* 2021; **374**: abe6474.
57. Tang F, Li J, Qi L *et al*. A pan-cancer single-cell panorama of human natural killer cells. *Cell* 2023; **186**: 4235–4251.e4220.
58. Yoshihara K, Shahmoradgoli M, Martínez E *et al*. Inferring tumour purity and stromal and immune cell admixture from expression data. *Nat Commun* 2013; **4**: 2612.

Supporting Information

Additional supporting information may be found online in the Supporting Information section at the end of the article.